Interdependence of groundwater dynamics and land-energy feedbacks under climate change

REED M. MAXWELL[1]*† AND STEFAN J. KOLLET[2]†

[1]Atmospheric, Earth and Energy Sciences Division, Lawrence Livermore National Laboratory (L-103), 7000 East Avenue, Livermore, California 94550, USA

[2]Metereological Institute, Bonn University, Auf dem Huegel 20, 53121 Bonn, Germany

*Current address: Department of Geology and Geologic Engineering, Colorado School of Mines, Golden, Colorado 80401, USA

†e-mail: rmaxwell@mines.edu; stefan.kollet@uni-bonn.de

Published online: 28 September 2008; doi:10.1038/ngeo315

Climate change will have a significant impact on the hydrologic cycle, creating changes in freshwater resources, land cover and land–atmosphere feedbacks. Recent studies have investigated the response of groundwater to climate change but do not account for energy feedbacks across the complete hydrologic cycle[1,2]. Although land-surface models have begun to include an operational groundwater-type component[3–5], they do not include physically based lateral surface and subsurface flow and allow only for vertical transport processes. Here we use a variably saturated groundwater flow model with integrated overland flow and land-surface model processes[6–8] to examine the interplay between water and energy flows in a changing climate for the southern Great Plains, USA, an important agricultural region that is susceptible to drought. We compare three scenario simulations with modified atmospheric forcing in terms of temperature and precipitation with a simulation of present-day climate. We find that groundwater depth, which results from lateral water flow at the surface and subsurface, determines the relative susceptibility of regions to changes in temperature and precipitation. This groundwater control is critical to understand processes of recharge and drought in a changing climate.

The southern Great Plains region of the USA is an important agricultural region that has experienced severe droughts over the past century including the 'dust bowl' of the 1930s (ref. 9). This system is different from the mountain regions investigated previously (in, for example, refs 10–12), as it is characterized by little winter snowpack, rolling terrain and seasonal precipitation. There is evidence that whereas drought timing may depend on sea surface temperature, the length and depth of major droughts in the region depend on soil moisture conditions and land–atmosphere interactions[9,13–15].

There is a growing body of work on mountain hydrology and snowpack response to a changing climate, particularly in western North America (for example refs 10–12). Recent work has begun to investigate the impact of climate change on groundwater recharge and storage[1,2,16–18]. These studies have shown changes in groundwater recharge in response to climate change[1,2,17,18] and the role of groundwater in maintaining baseflow under an altered climate[16]. However, these studies have not included feedbacks from groundwater to the land surface, particularly the land-surface recently shown to be important[7,19].

Here, we study the response of a watershed in the southern Great Plains in Oklahoma, USA using a unique, integrated groundwater/surface-water/land-surface model. Perturbed forcing input is developed to represent plausible climate change scenarios and used to drive the coupled model. Results include both the watershed response, such as changes in soil moisture, recharge and water-table depth, and land-surface feedbacks including changes in the energy budget. Three future climate scenario simulations were generated by perturbing the control run (CNTRL) with the atmospheric conditions of the water-year 1999. All perturbations consisted of a systematic increase in air temperature by 2.5 K with (1) no precipitation change (H: hot), (2) an increase in precipitation by 20% (HW: hot and wet) and (3) a decrease in precipitation by 20% (HD: hot and dry). These perturbations were meant to represent the variability and uncertainty in regional changes to central North America under global simulations of future climate[20].

Figure 1 shows yearly averaged saturation, water-table depth, potential recharge, ground surface temperature and latent heat flux for CNTRL and the difference for each scenario minus CNTRL. This figure shows that, in general, the saturation decreases slightly for H (Fig. 1b1), increases for HW (Fig. 1c1) and decreases significantly for HD (Fig. 1d1). Closer inspection reveals that the soil moisture does not change in the river valleys, even for the dry scenario HD (Fig. 1d1). This is due to lateral subsurface redistribution of water, which converges in the valleys, maintaining soil moisture at higher values. These patterns of surface–subsurface interplay are reinforced by viewing the water-table depth and differences (Fig. 1a2–d2). Figure 1a2 clearly shows the river valleys as the dark blue regions with values of water-table depth less than two metres. These panels show no difference in water-table depth in the river valleys between the scenarios and CNTRL; however, there is an increase in water-table depth especially along the hillslopes in scenarios H (Fig. 1b2) and HD (Fig. 1d2) and a decrease in water-table depth in HW (Fig. 1c2).

The plots of potential recharge, precipitation minus total evaporation and transpiration ($P - E$), in Fig. 1a3–d3 demonstrate significant spatial variability in all cases. This figure indicates that potential recharge is negative in the river valleys in all cases (upward flux), whereas recharge elsewhere is positive in CNTRL (Fig. 1a3), negative in H (Fig. 1b3), positive in HW (Fig. 1c3) and strongly negative in HD (Fig. 1c4).

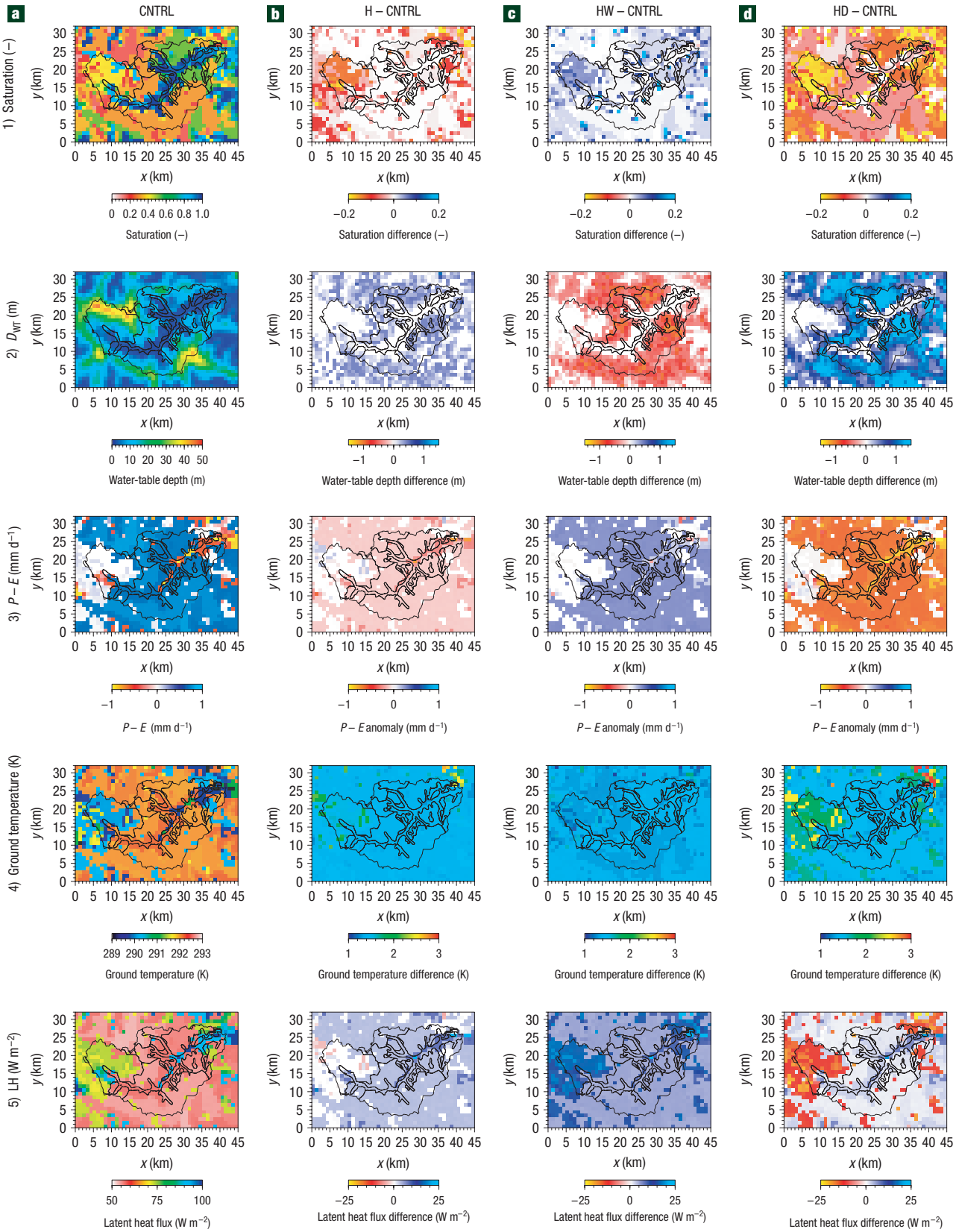

Figure 1 Spatial distribution of yearly averaged water and energy components from CNTRL and scenario calculations. Plot of yearly averaged saturation (1), water-table depth (2), potential recharge (3), ground surface temperature (4) and latent heat flux (5) for CNTRL (**a**) and differences between H (**b**), HW (**c**) and HD (**d**) and CNTRL for each of the variables. Note the watershed outline plotted on each panel. Individual panels are referred to as a number–letter grid (for example, **a**1 for CNTRL saturation). Note that recharge is potential, that is $P-E$, which excludes runoff.

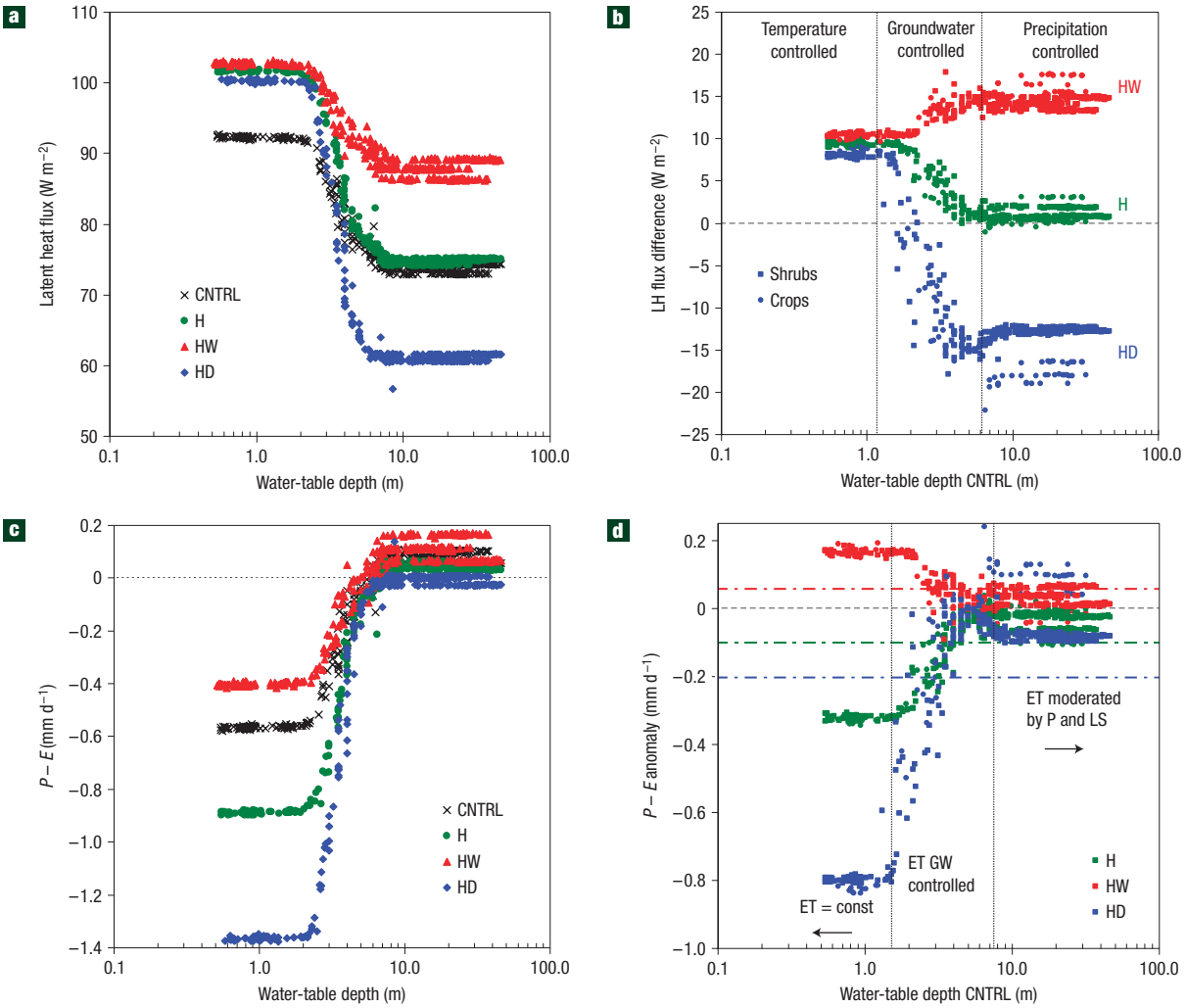

Figure 2 Semi-logarithmic plots of latent heat and *P* − *E* as a function of water-table depth. a–d, Yearly averaged latent heat flux (**a**) and latent heat flux difference (**b**) as a function of the water-table depth of CNTRL for each of the scenario cases as indicated and *P* − *E* (**c**) and *P* − *E* anomaly (**d**) as a function of water-table depth for two vegetation types as indicated in **b**. Spatial averages of *P* − *E* anomaly are shown for each scenario by the dashed lines of corresponding colour to the symbols. ET = evapotranspiration, P = precipitation, LS = land − surface processes, GW = groundwater. Each symbol represents a yearly averaged spatial location (pixel) in the model domain.

In Fig. 1, plots of ground temperature (Fig. 1a4–d4) are also spatially heterogeneous owing to convergent flow and spatially distributed vegetation and soil cover. This figure shows that for scenario H (Fig. 1b4), yearly averaged increases in ground surface temperature are greater than the increases seen from scenario HW (Fig. 1c4) but not as great as HD (Fig. 1d4). Scenario HD shows a clear influence of convergent groundwater flow in the river valleys with smaller temperature increases corresponding spatially to locations with small groundwater and saturation differences. Figure 1a5–d5 also shows that latent heat fluxes vary spatially with larger values in the river valleys than along hilltops. All scenarios show further increases in latent heat flux in the river valleys (Fig. 1b5–d5). Outside the river valleys, scenario H (Fig. 1a5) shows slight increases in latent heat fluxes, HW (Fig. 1c5) shows strong increases (Fig. 1b5) and HD (Fig. 1d5) shows moderate to strong decreases.

Careful inspection of Fig. 1 reveals that much of the variability in recharge and energy fluxes seems to be spatially correlated with groundwater depth. Figure 2 explores this spatial variability further, plotting yearly averaged latent heat flux, latent heat flux difference, potential recharge and potential recharge anomaly as a function of water-table depth for all cases. In the river valleys, where groundwater is shallow, latent heat fluxes are largest (Fig. 2a) and recharge is negative (Fig. 2c), owing to a constant supply of water to the land surface. Conversely, where groundwater is deep we see the smallest values of latent heat flux (Fig. 2a) and recharge (Fig. 2b) owing to water limitations at the land surface. Figure 2a,c also shows that for groundwater depths between two and five metres, there is a strong correlation between recharge and latent heat flux and water-table depth. These relationships have been explored previously[7] and this region is the so-called critical zone where subsurface and land-surface processes are most tightly coupled.

Figure 2b also shows a significant impact of groundwater on latent heat flux differences between the scenarios and the control. This figure shows very little difference between scenarios for shallow water-table depths and the largest differences at great water-

table depth. In the river valley, all scenarios show an increase in latent heat flux at small water-table depths due to the uniform increase in temperature. At large water-table depths (at the hill tops), we see large differences in latent heat flux due to differences in precipitation. This is reinforced by HW having a large positive difference in latent heat flux, HD a large negative difference and H (with the same rainfall as CNTRL) almost no difference. In the critical zone, where groundwater depths range from two to five metres, we again see a strong correlation between water-table depth and difference in latent heat flux, indicating the control groundwater exerts on the watershed response as a consequence of the climate change scenarios.

Figure 2d shows that the $P-E$ anomaly (difference in potential recharge between each scenario and CNTRL) depends on water-table depth as well. At shallow depths, the $P-E$ anomaly is due to differences in precipitation as evapotranspiration is very similar in all scenarios, shown in Fig. 2a. For a deeper water table, there is less variability in the $P-E$ anomaly between scenarios and more scatter in the curves. This scatter is due to differences in land cover and soil type and the $P-E$ anomaly is due to a combination of the differences in parameters for these soil and vegetation types and rainfall amount. Again we see a strong dependence of the $P-E$ anomaly on groundwater depth in the critical zone between two and five metres. At large water-table depths, groundwater is disconnected from the land surface and the land surface is in dynamic equilibrium with atmospheric forcing. These equilibrium conditions would be expected over the entire model domain from traditional land-surface models that lack lateral subsurface flow. This is particularly important because the spatial variability in water-table depth significantly affects the spatial average in the $P-E$ anomaly, shown by the coloured horizontal lines for each case. These average $P-E$ anomalies show strong drought conditions for H ($-0.1\,\mathrm{mm\,d^{-1}}$), comparable to the 'dust bowl' of the 1930s and the drought in the 1950s (ref. 21). HW demonstrates an increase in $P-E$ anomaly and HD shows a significant decrease in $P-E$ anomaly ($-0.2\,\mathrm{mm\,d^{-1}}$) twice the value of any drought on record in the region over the past century. Figure 2d clearly shows that the severity of the basin-averaged drought conditions would be significantly underestimated by land-surface processes alone, without the inclusion of lateral groundwater flow.

In Fig. 2a,b, the large annual changes in latent heat flux also indicate the potential for land–atmosphere feedbacks for scenarios H and HD. Both cases show an increase in latent heat flux in the river valley and either no change or a significant decrease in latent heat flux at the hill tops. Previous work has documented the potential for land–atmosphere feedbacks[19,22,23] and the current simulations indicate that these feedbacks would be amplified. One of these studies[19] has shown a connection specifically between groundwater and atmospheric processes (for example, the effects of water-table depth on potential temperature, wind and the growth of the atmospheric boundary layer), providing an even stronger basis for inclusion of groundwater and lateral flow in simulations of climate change. The strong convective conditions created by large spatial energy flux gradients could indeed feed back to maintain dry conditions[24].

In summary, this study uses an integrated watershed model with coupled hydrology and land-surface energy components to investigate watershed response, interactions and feedbacks from future climate scenario simulations. It is shown that groundwater storage acts as a moderator of watershed response and climate feedbacks. In zones with a shallow water table, the changes in land-surface energy fluxes are primarily a function of atmospheric temperature increase, as these processes are never water limited. In areas where the water table is deep, changes in land-surface energy fluxes are mostly a function of precipitation because there is little feedback from groundwater. In the so-called critical zone[7], between two and five metres depth in this study, very strong correlations between water-table depth and land-surface energy response are demonstrated. These findings also have strong implications for drought as $P-E$ anomalies also demonstrate a strong dependence on areas of convergent flow and water-table depth. These findings suggest that the energy feedbacks from the land surface could impart a significant signal in the lower atmosphere, which might in turn modify atmospheric response. Although the area studied is regional in size, the results suggest that the role of lateral subsurface flow should not be ignored in climate-change simulations and drought analysis.

METHODS

The model ParFlow was used in this study. It is a fully integrated, parallel watershed model[6–8,19,25,26] and is capable of simulating fluid and mass transport processes in the deep subsurface, the vadose zone, root zone and land surface. This includes integrated overland flow (river and hillslope flow[6]) and a land-surface model, CLM[7,8,27], which accounts for energy and plant processes at the land surface.

ParFlow was applied to the Little Washita watershed in Oklahoma, USA and the model domain was 45 km × 32 km. The simulations used a 1 km lateral and 0.5 m vertical discretization with a very deep subsurface (∼100 m) to fully capture both shallow subsurface and deeper groundwater lateral flow[7]. The spatially heterogeneous soil of the watershed is mostly loamy sand, sand, with some sand and silt loam. The watershed is rolling terrain covered by grass with shrubs and interspersed trees. The elevation, soil and vegetation cover data for this domain have been previously published[7,19].

Four equilibrium simulations were conducted: one control based on current and three perturbations based on future global climate model predictions (ref. 20, Table 11.1). The simulation of the current climate scenario (CNTRL) based on water-year 1999 is documented in ref. 7. In CNTRL, spatially uniform atmospheric forcing derived from North American Regional Reanalysis for water-year 1999 was linearly interpolated to one hour intervals to create a continuous time series of precipitation, air temperature, downward solar radiation, air pressure, wind and relative humidity.

The three future climate scenario simulations were generated by perturbing the water-year 1999 time series. The perturbations consisted of (1) a systematic increase in air temperature by 2.5 K with all other forcing variables unchanged (H), (2) an increase in air temperature by 2.5 K with an increase in precipitation by 20% (HW) and (3) an increase in temperature by 2.5 K with a decrease in precipitation by 20% (HD). Each of the scenarios was spun-up, that is, started from the CNTRL state and forced repeatedly with the perturbed data set until changes in the mass and energy balance over the year dropped below a threshold. All simulations were carried out on the LLNL system Thunder, a 4,096-processor 64-bit parallel computer. Twenty cpus were used per simulation case and a spin-up time of three years was required.

Received 12 June 2008; accepted 28 August 2008; published 28 September 2008.

References

1. Allen, D. M., Mackie, D. C. & Wei, M. Groundwater and climate change: A sensitivity analysis for the Grand Forks aquifer, southern British Columbia, Canada. *Hydrogeol. J.* **12**, 270–290 (2004).
2. Scibek, J. & Allen, D. M. Modeled impacts of predicted climate change on recharge and groundwater levels. *Wat. Resour. Res.* **42**, W11405 (2006).
3. Gulden, L. E. *et al.* Improving land-surface model hydrology: Is an explicit aquifer model better than a deeper soil profile? *Geophys. Res. Lett.* **34**, L09402 (2007).
4. Liang, X., Xie, Z. H. & Huang, M. Y. A new parameterization for surface and groundwater interactions and its impact on water budgets with the variable infiltration capacity (VIC) land surface model. *J. Geophys. Res.-Atmos.* **108**, 8613 (2003).
5. Yeh, P. J. F. & Eltahir, E. A. B. Representation of water table dynamics in a land surface scheme. Part I: Model development. *J. Clim.* **18**, 1861–1880 (2005).
6. Kollet, S. J. & Maxwell, R. M. Integrated surface-groundwater flow modeling: A free-surface overland flow boundary condition in a parallel groundwater flow model. *Adv. Wat. Resour.* **29**, 945–958 (2006).
7. Kollet, S. J. & Maxwell, R. M. Capturing the influence of groundwater dynamics on land surface processes using an integrated, distributed watershed model. *Wat. Resour. Res.* **44**, W02402 (2008).
8. Maxwell, R. M. & Miller, N. L. Development of a coupled land surface and groundwater model. *J. Hydrometeorol.* **6**, 233–247 (2005).
9. Schubert, S. D. *et al.* Potential predictability of long-term drought and pluvial conditions in the US Great Plains. *J. Clim.* **21**, 802–816 (2008).
10. Cayan, D. R. *et al.* Climate change scenarios for the California region. *Clim. Change* **87**, S21–S42 (2008).
11. Dettinger, M. D. *et al.* Simulated hydrologic responses to climate variations and change in the Merced, Carson, and American River basins, Sierra Nevada, California, 1900–2099. *Clim. Change* **62**, 283–317 (2004).

12. Vanrheenen, N. T. *et al.* Potential implications of PCM climate change scenarios for Sacramento-San Joaquin River Basin hydrology and water resources. *Clim. Change* **62**, 257–281 (2004).
13. Hong, S. Y. & Kalnay, E. Role of sea surface temperature and soil-moisture feedback in the 1998 Oklahoma-Texas drought. *Nature* **408**, 842–844 (2000).
14. Hong, S. Y. & Kalnay, E. The 1998 Oklahoma-Texas drought: Mechanistic experiments with NCEP global and regional models. *J. Clim.* **15**, 945–963 (2002).
15. Schubert, S. D. *et al.* On the cause of the 1930s dust bowl. *Science* **303**, 1855–1859 (2004).
16. Tague, C. *et al.* Deep groundwater mediates streamflow response to climate warming in the Oregon Cascades. *Clim. Change* **86**, 189–210 (2008).
17. Scibek, J. *et al.* Groundwater-surface water interaction under scenarios of climate change using a high-resolution transient groundwater model. *J. Hydrol.* **333**, 165–181 (2007).
18. York, J. P. *et al.* Putting aquifers into atmospheric simulation models: An example from the Mill Creek Watershed, northeastern Kansas. *Adv. Wat. Resour.* **25**, 221–238 (2002).
19. Maxwell, R. M., Chow, F. K. & Kollet, S. J. The groundwater-land-surface-atmosphere connection: Soil moisture effects on the atmospheric boundary layer in fully-coupled simulations. *Adv. Wat. Resour.* **30**, 2447–2466 (2007).
20. Christensen, J. H. *et al.* in *Climate Change 2007: The Physical Science Basis. Contribution of Working Group I to the Fourth Assessment Report of the Intergovernmental Panel on Climate Change* (eds Solomon, S. *et al.*) (Cambridge Univ. Press, Cambridge, 2007).
21. Seager, R. *et al.* Model projections of an imminent transition to a more arid climate in southwestern North America. *Science* **316**, 1181–1184 (2007).
22. Chen, F. & Avissar, R. The impact of land-surface wetness heterogeneity on mesoscale heat fluxes. *J. Appl. Meteorol.* **33**, 1323–1340 (1994).
23. Patton, E. G., Sullivan, P. P. & Moeng, C. H. The influence of idealized heterogeneity on wet and dry planetary boundary layers coupled to the land surface. *J. Atmos. Sci.* **62**, 2078–2097 (2005).
24. Seiffert, R. & von Storch, J.-S. Impact of atmospheric small-scale fluctuations on climate sensitivity. *Geophys. Res. Lett.* **25**, L10704 (2008).
25. Jones, J. E. & Woodward, C. S. Newton–Krylov–multigrid solvers for large-scale, highly heterogeneous, variably saturated flow problems. *Adv. Wat. Resour.* **24**, 763–774 (2001).
26. Ashby, S. F. & Falgout, R. D. A parallel multigrid preconditioned conjugate gradient algorithm for groundwater flow simulations. *Nucl. Sci. Eng.* **124**, 145–159 (1996).
27. Dai, Y. J. *et al.* The common land model. *Bull. Am. Meteorol. Soc.* **84**, 1013–1023 (2003).

Acknowledgements

This work carried out under the auspices of the US Department of Energy by Lawrence Livermore National Laboratory under Contract DE-AC52-07NA27344 and was supported by the LLNL Climate Change Initiative.

Author information

Reprints and permission information is available online at http://npg.nature.com/reprintsandpermissions.
Correspondence and requests for materials should be addressed to R.M.M. or S.J.K.